



HAL
open science

Biomechanical wall properties of human intracranial aneurysms resected following surgical clipping

Vincent Costalat, Mathieu Sanchez, Dominique Ambard, L. Thines, Nicolas Lonjon, Franck Nicoud, H. Brunel, J.P. Lejeune, Henri Dufour, P. Bouillot, et al.

► **To cite this version:**

Vincent Costalat, Mathieu Sanchez, Dominique Ambard, L. Thines, Nicolas Lonjon, et al.. Biomechanical wall properties of human intracranial aneurysms resected following surgical clipping. *Journal of Biomechanics*, 2011, 44 (15), pp.2685-2691. 10.1016/j.jbiomech.2011.07.026 . hal-00686616

HAL Id: hal-00686616

<https://hal.science/hal-00686616v1>

Submitted on 24 Apr 2012

HAL is a multi-disciplinary open access archive for the deposit and dissemination of scientific research documents, whether they are published or not. The documents may come from teaching and research institutions in France or abroad, or from public or private research centers.

L'archive ouverte pluridisciplinaire **HAL**, est destinée au dépôt et à la diffusion de documents scientifiques de niveau recherche, publiés ou non, émanant des établissements d'enseignement et de recherche français ou étrangers, des laboratoires publics ou privés.

1 Biomechanical wall properties of human intracranial
2 aneurysms resected following surgical clipping
3 **(IRRA Project*)**
4
5

6 V. Costalat, M. Sanchez, D. Ambard, L. Thines, N. Lonjon, F. Nicoud, H. Brunel, J.P. Leje-
7 une, H. Dufour, P. Bouillot, JP Lhaldky, K. Kouri, F. Segnarbieux, CA Maurage, K. Lobote-
8 sis, M.C. Villa-Uriol, C. Zhang, A.F. Frangi, G. Mercier, A. Bonafé, L. Sarry, and F. Jourdan.

9
10 * The research consortium “**Individual Risk Rupture Assessment of Intracranial aneurysm**”
11 (IRRA) was founded by 4 clinical centers, and 3 European laboratories in France, and Spain.
12
13

14 **Classification = Original Research**

15
16 **Word count:** Main Text and Abstract = 2829
17

18
19 BM-D-11-00205
20
21

22 **Contact information:**

23 Vincent Costalat, MD, PhD (vincentcost@hotmail.com)

24 CHU Montpellier, Interventional Neuroradiology, Av Augustin Fliche, Montpellier, France.
25
26
27

27

28

29 **All authors have made substantial contributions to all of the following:**

30 (1) the conception and design of the study; VC;DA;FJ;FN;MS

31 (2) acquisition of data; VC;MS; LT;NL;JPL;FS;HD;HB;PB;JPH;CAM;KK;AB

32 (3) analysis and interpretation of data; GM;VC;FJ;DA;MS

33 (4) drafting the article or revising it critically for important intellectual content;

34 VC;MS;FJ;KL;DA;FN;LS;AFF

35

35

36

37

38

38

39 **Abstract:**

40 **Background and Purpose**— Individual rupture risk assessment of intracranial aneurysms is a
41 major issue in the clinical management of asymptomatic aneurysms. Aneurysm rupture occurs
42 when wall tension exceeds the strength limit of the wall tissue. At present, aneurysmal wall
43 mechanics are poorly understood and thus, risk-assessment involving mechanical properties is
44 inexistent. Additionally, aneurysmal computational hemodynamics usually makes the as-
45 sumption of rigid walls, an arguable simplification. We therefore aim to assess mechanical
46 properties of ruptured and unruptured intracranial aneurysms in order to provide the founda-
47 tion for future patient-specific aneurysmal risk assessment. This work will also challenge
48 some of the currently held hypotheses in computational flow hemodynamics research.

49 **Methods**—A specific conservation protocol was applied to aneurysmal tissues following clip-
50 ping and resection in order to preserve their mechanical properties. **Sixteen intracranial** an-
51 eurysms (11 female, 5 male) underwent mechanical uni-axial stress tests under physiological
52 conditions, temperature, and saline isotonic solution. These represented 11 unruptured and 5
53 ruptured aneurysms. Stress/strain curves were then obtained for each sample, and a fitting
54 algorithm was applied following a 3-parameter (C^{10} , C^{01} , C^{11}) Mooney-Rivlin hyperelastic
55 model. Each aneurysm was classified according to its biomechanical properties and
56 (un)rupture status.

57 **Results**— Tissue testing demonstrated three main tissue classes: Soft, Rigid, and Intermedi-
58 ate. All unruptured aneurysms presented a more Rigid tissue than ruptured or pre-ruptured
59 aneurysms within each gender subgroup. Wall thickness was not correlated to aneurysmal
60 status (ruptured/unruptured). An Intermediate subgroup of unruptured aneurysms with softer
61 tissue characteristic was identified and correlated with multiple documented risk factors of
62 rupture.

63 **Conclusion: A significant biomechanical properties modification between ruptured an-**
64 **eurysm, presenting a soft tissue and unruptured aneurysms, presenting a rigid material**
65 **was observed. This finding strongly supports the idea that a biomechanical-based risk**
66 **factor can and should be developed in the near future to improve the therapeutic deci-**
67 **sion making.**

68

68

69

70 **Introduction:**

71 The prevalence of unruptured intracranial aneurysms in the general population, as reported by
72 a recent review,¹ ranges between 3% and 6.6%. The incidence of ruptured aneurysms is how-
73 ever, low, with approximately 0.5% per year suggesting that very few aneurysms rupture.
74 Subarachnoid hemorrhage is the consequence of aneurysm rupture and approximately 12% of
75 patients die before receiving medical attention, 40% of hospitalized patients die within one
76 month after the event, and more than one third of those who survive have major neurological
77 deficits. In contrast endovascular treatment of unruptured aneurysms is safe with less than 1%
78 mortality rate². Unruptured intracranial aneurysms represent a dilemma for the physicians.
79 The risks of aneurysm rupture with respect to its natural history against the risk of morbidity
80 and mortality from an endovascular or surgical repair has to be carefully balanced. With brain
81 imaging being more frequently and widely used, a growing number of intracranial aneurysms
82 are being diagnosed, posing the problem of which aneurysms harbor a sufficiently high risk of
83 rupture to merit endovascular or surgical repair. Recent publications have addressed this issue
84 and have demonstrated that, among other variables affecting the natural history of aneurysms,
85 aneurysm size and location represent independent predictors of rupture risk³. Other param-
86 eters, such as irregular aneurysm shape and, in particular, the presence of blebs^{4, 5} are recog-
87 nized as high risk factors.

88 Rupture of an aneurysm occurs when wall tension exceeds the strength limit of the wall tis-
89 sue. The ideal approach to risk assessment would therefore be to determine tension and mate-
90 rial strength limits of the tissue⁶ in the aneurysmal wall. Individual aneurysmal material
91 strength is impossible to measure non-invasively, but wall tension can be estimated using
92 computational simulation⁷. Over the last decade, a number of authors have shown that com-
93 putational fluid dynamic simulations based on patient-specific anatomical models derived
94 from medical imagery may be used to assess wall shear stress (WSS) and pressure in the Cir-
95 cle of Willis^{8, 9, 10}. Others have used the same approach to analyze cerebral aneurysms, with
96 particular focus on WSS, which is thought to be associated with aneurysm formation and risk
97 rupture.^{11, 12, 13} Although simulation of aneurysmal wall tension is now feasible in principle,
98 real human aneurysmal wall biomechanical properties are still rarely explored in the litera-
99 ture.^{14, 15} Computational simulations must be based on reliable material properties and

100 boundaries. As opposed to hemodynamic boundary conditions that may be assessed by Phase
101 Contrast-MRI or transcranial Doppler, in vivo, patient specific measurements of tissue prop-
102 erties are not feasible yet. Most of the current research on computational hemodynamics
103 assumes uniform wall thickness and wall properties based on average values extracted from
104 the scarce available literature. Although some of these assumptions may be acceptable in
105 practice, no in-depth study has demonstrated their validity thus casting shadows on the accu-
106 racy of the current computational hemodynamics work. For this purpose a research consor-
107 tium (**IRRAs** for **I**ndividual **R**isk **R**upture **A**ssessment of Intracranial Aneurysm) was
108 founded between 3 research Laboratories and 4 French neurosurgical centers (Montpellier,
109 Lille, Nimes and Marseille) and involving corresponding departments of neuroradiology and
110 anatomopathology. The first purpose of the **IRRAs** consortium is to build a database of aneu-
111 rysmal biomechanical parameters. Such database will be instrumental in supporting new
112 computational strategies to determine the risk of rupture in cerebral aneurysms based on pa-
113 tient-specific imaging data and domain-specific biomechanical knowledge.

114 **The purpose of this study is to explore the biomechanical behavior characteristics of**
115 **ruptured and unruptured aneurysms. Building such database is a mandatory to estab-**
116 **lish the idea that the rheology of the tissue correlates with the status of the aneurysm**
117 **and that a biomechanical-based risk rupture factor can indeed be developed.**

118

118

119 **Materials and methods**

120 *Surgical technique and aneurysm selection*

121 Eighteen patients treated for ruptured or unruptured aneurysms by surgical clipping were re-
122 cruited by 4 French neurosurgical teams. The research study protocol was approved by the
123 local ethical committee in each center. A consent form was signed by patients with normal
124 neurological status, or by the relatives in all other cases. Following surgical clipping (Fig.1)
125 angio fluoroscopy imaging was performed by the neurosurgeon to control aneurysm sac ex-
126 clusion. Once the distal aneurysm was confirmed to be safely excluded from the circulation,
127 the neurosurgeons removed it in one piece. In this way, 18 intact aneurysms samples were
128 then extracted from 17 patients.

129 *Clinical and Radiological Data*

130 **For each patient, clinical, and radiological information was collected concerning age,**
131 **gender, aneurysm status (ruptured/unruptured), size (measured from the dome of the**
132 **aneurysm and the neck represented by the communication of the aneurysm with the**
133 **parent artery), the “dome to neck” ratio (aneurysm size/neck length), location on the**
134 **Willis circle, morphological evaluation (classified "simple shaped" for regular unilobu-**
135 **lated aneurysm and "complex shaped" for multilobulated and irregular aneurysm), as**
136 **well as documented rupture risk factors; multiple aneurysms, previous ruptured aneu-**
137 **rysm, positive family history of ruptured intracranial aneurysm, autosomal dominant**
138 **polycystic kidney disease, hypertension, alcohol and tobacco.** A possible mycotic intracra-
139 nial aneurysm etiology was considered an exclusion criterion, as well as any previous history
140 of endocarditis and inflammatory disease. **All documented risk factors were then recorded**
141 **in order to be related to the biomechanical behavior of each aneurysm.**

142 *Aneurysm Sample Conservation protocol*

143 In order to conserve the mechanical properties of the aneurysm wall, a specific conservation
144 protocol was applied in each center by means of a dedicated histopathological removal kit
145 available in the neurosurgical operating room. The resected aneurysm was initially inserted in
146 a tube containing a Ringer lactate, 10% DMSO solution. This first tube was then placed in a
147 larger second one containing isopropanol. This combination of the two tubes was placed in a
148 freezer (-80°C). The sample was progressively frozen due to the surrounding isopropanol so-
149 lution in order to maintain its biomechanical properties¹⁶. Frozen samples were then stored in

150 the anatomopathology department of the neurosurgical center, before mechanical testing was
151 carried out.

152

153 *Biomechanical testing methodology*

154 One hour before mechanical testing, aneurysms sample were thawed at ambient temperature.
155 Under microscopy, the aneurysmal wall samples were dissected in a meridional manner in
156 order to obtain a regular rectangular piece (Fig.2). **Only the meridional axis of the**
157 **aneurysm was chosen in order to preserve maximum length of the aneurysmal tissue in**
158 **the sample given the very small size of each specimen and the fragility of the tissue.** The
159 aneurysm strips were physically measured and then glued on each extremity to aluminum
160 grips. Meanwhile, physiological isotonic liquid was warmed to 40°C inside the traction test
161 machine. A uniaxial stretch test was carried out on the sample within the warmed
162 physiological liquid in order to simulate the in vivo conditions (Fig. 3a). This testing device
163 was composed of a Texture Analyzer (TA-XT2, Stable Microsystems, UK) with a 50 N load
164 cell and an optical microscope (ZEISS) equipped with a digital video camera .

165 The uniaxial stretch test consisted of a sequence of 10% length displacement of the sample, in
166 5 repeated cycles (Fig. 3b), while registering the traction force applied. This 10% value was
167 initially calculated by Karmonik et al.¹⁷ in an in-vivo wall motion MRI study of 7 aneurysms.
168 **In accordance to standard mechanical testing protocol for biological tissue, the speci-**
169 **mens were first preconditioned¹⁸ during the first four cycles.** The extension rate was 0.01
170 mm/s and the tension load was recorded every 0.01 s. Velocity of the solicitations was small
171 enough to not consider viscous phenomena. A baseline tension of 0 Newton was applied to
172 the strip before starting each test, and two cameras were orthogonally placed and focused on
173 the sample after a calibration test

174 During the test, the two subset cameras were used to record the displacement of the sample.
175 These images were subsequently used to determine the exact **dimensions** of the strips (resolu-
176 tion of 4µm/pixel). A Force/Displacement graph was obtained **from each sample testing al-**
177 **lowing tissue characterization**

178

178 **Post processing**

179 Only the measurements from the last elongation cycle were used in order to obtain more real-
180 istic mechanical characterization of the data. Note however that except for the very first cycle,
181 the force/displacement graph was roughly cycle independent (fig 3 b).. In order to tune the
182 parameters of an equivalent hyperelastic model, the force/displacement graph described
183 above was converted in a strain/stress graph. For this calculation, the length, thickness and
184 width of each strip were considered (Fig. 3b). A baseline for this aneurysmal **strip dimen-**
185 **sions** were obtained at 0-Newton traction in the third cycle of each test. Using the assumption
186 that the specimen was subjected to a uniform traction and presented a constant section during
187 the test, the Cauchy stress was computed, and the engineering strain registered^{19, 20}.

188 During the cycles some permanent deformation in the traction phase was observed causing
189 slight compression of the sample in the rest phase. This is reflected by the negative values of
190 the curve origin in Figure 3b and is in accordance to the elasto-plastic behavior of the tissue.
191 Since we consider an hyperelastic model to represent the tissue, the (moderate) plastic effects
192 cannot be represented and only the positive part of the curve was used to identify material
193 behavior.

194 Once the strain/stress graph was obtained, we proceed to a mathematical matching using a
195 Sequential Least Squares Programming algorithm in order to determine the corresponding
196 hyperelastic model and its coefficients. In our cases, the best match was obtained with a 3
197 parameters Mooney-Rivlin model^{21, 22}. Let F be the measured load, S_0 the initial section and λ
198 the elongation of the sample, the behavior law is given by equation (1)..

$$199 \quad (1) \quad \frac{F}{S_0} = 2(\lambda - \lambda^{-2}) \left(c_{10} + c_{01} \lambda^{-1} + c_{11} (3\lambda^{-2} + 3\lambda - 3 - 3\lambda^{-1}) \right)$$

200 where the material parameters are C_{10} , C_{01} and C_{11} . The values of each of these
201 coefficients for each aneurysm are gathered in Table 1 together with **strip dimensions**
202 and relevant clinical factors.

203 **Statistical analysis**

204 The aneurysmal wall characteristics were presented using median and range for continuous
205 variables and frequencies and proportions for categorical variables. Groups (defined by
206 biomechanical status and material property) were compared using non-parametric Wilcoxon

207 rank test for continuous variables and Fisher exact test for categorical ones. Statistical
208 significance threshold was set at 5%. Statistical analyses were performed using SAS version
209 9.1 (SAS Institute, Cary, North Carolina).

210

211 **Results:**

212 ***Population:***

213 Eleven unruptured and five ruptured aneurysms were included in the study. In one unruptured
214 aneurysm case, pre-rupture symptoms with acute headache, and recent vision loss secondary
215 to optic nerve compression was reported and highlighted in the table 1. Mean age was 46.7
216 (min 32 – max 64). Location was middle cerebral artery (MCA) in 9 cases (56.6%), anterior
217 communicant artery (AComA) in 3 cases (18.7%), posterior communicant artery (PComA) in
218 2 cases (12.5%), and internal carotid artery (ICA) in 2 cases (6%). Aneurysm size is ranging
219 from 4.2 to 13 mm.

220 ***Sample and Mechanical testing:***

221 Out of the 16 surgically clipped aneurysms that were subjected to mechanical uniaxial strain
222 tests, 11 were from female and 5 from male patients (Sex Ratio = 0.45). Mean strip length
223 was 4.8 mm (ranging from 1.3 to 8), with a mean thickness of 370 μm (ranging from 170 to
224 680 μm), and a mean section surface of 0.62 mm^2 (ranging from 0.29 to 1.6 mm^2).

225 The coefficient C_{10} value ranged from 0 to 0.9 Mpa with a mean value of 0.19 Mpa, C_{01}
226 ranged from 0 to 0.13 Mpa with a mean value of 0.024, C_{11} ranged from 0.124 to 32 Mpa
227 with a mean value of 7.87.

228 To facilitate analysis, aneurysms were classified according to their status Ruptured/
229 Unruptured and their biomechanical behavior Rigid/Soft/Intermediate (see Tables 1 and
230 2).

231

232 ***Comparison of biomechanical parameters value among ruptured and unruptured aneu-***
233 ***rysms are summarized in tables 3, 4, and 5.***

234

235

236

237

238 **Discussion**

239 ***Results analysis***

240 A recent case-control study²³ on 4000 patients based on genetic variation suggests
241 that the underlying mechanism for intracranial aneurysm pathogenesis may differ between
242 male and female subjects, underlining the importance of a stratified analysis between genders.
243 A significant difference in biomechanical parameters between ruptured and unruptured aneu-
244 rysms was observed in our data within each gender group (Tables 3, 4, 5), therefore support-
245 ing the above statement.

246 Interestingly, the C_{11} coefficient, which represents the main curvature of each graph was the
247 most representative parameter of this observed biomechanical difference (Table 3, $p < 0.004$).
248 The first two coefficients C_{01} , C_{10} presented a low value (near 0) and were not significantly
249 different ($p = 0.4$ and $p = 0.7$) regarding aneurysmal status (ruptured/unruptured). All C_{11} values
250 were observed below 1.2 MPa (mean 0.37 MPa) in ruptured or pre ruptured female aneu-
251 rysms, and below 3.2MPa (mean 3.1MPa) in male ruptured aneurysms.

252 In the female group, all the unruptured aneurysms presented a more rigid behavior
253 than the ruptured or pre-ruptured aneurysms ($C_{11} = 0.48$ vs 11.7 MPa; $p < 0.001$, Table 4). Be-
254 tween the unruptured aneurysms, we can distinguish two subgroups; the Unruptured/Rigid
255 patients (#2-#7-#9) and the Unruptured/Intermediate patients (#8-#10-#11-#15). In this last
256 subgroup representing an unruptured aneurysm with a softer aneurysmal wall, three out of
257 four presented either documented major epidemiologic risk factors or a radiologically high
258 risk shape (multilobulated). Only one aneurysm (#15) was simple shaped without further as-
259 sociated risk factors in this subgroup. One single patient (#16) presenting an unruptured aneu-
260 rysm was classified as Soft with similar material properties with the Ruptured group. In this
261 particular case, pre-rupture symptoms with major headache, and recent optic nerve compres-
262 sion were recorded few days before surgery and motivated urgent treatment. Therefore, in this
263 case, the mechanical test findings of Soft may not be as paradoxical as thought of at the first
264 glance.

265 In the male group, all the unruptured aneurysms tended have Rigid material than the
266 ruptured ones ($C_{11} = 11.95$ vs 3.17 MPa; $p = 0.058$, Table 5). Similarly to the female, unrup-
267 tured aneurysms can be split in two subgroups, with 2 aneurysms classified Unrup-
268 tured/Intermediate (Aneurysm #12 and #14), and one aneurysm classified Unruptured/Rigid.
269 Among the Intermediate/Unruptured aneurysms one presented a major documented risk factor
270 with multiple aneurysms, in accordance to a possible underlying connective tissue disease.
271 Interestingly, in the male group, the ruptured aneurysms (Aneurysms #5 and #13) had a
272 thicker wall compared to the Intermediate/Unruptured aneurysms, in contradiction to common
273 conceptions, and in accordance to previous histopathologic work²⁴.

274 **Rheological data relevant to aneurysmal tissue are very scarce in the literature.**
275 **To the authors' knowledge, the only previous study is by Toth et al. ²² who also gained**
276 **insights about the tissue rheology from 1D traction testing. Unfortunately, no subgroup**
277 **analysis among ruptured or unruptured status was performed by Toth et al. and the**
278 **significant parameter C_{11} was not calculated. Still, the initial mean tangent modulus they**
279 **obtained for their hyperelastic model can be compared to the $C_{01}+C_{10}$ parameter from the**
280 **previous study. For the women group, this initial tangent modulus was evaluated from**
281 **$2.79 \cdot 10^{-2}$ to $22.4 \cdot 10^{-2}$ Mpa vs whereas it is in the range $1.905 \cdot 10^{-2}$ to $77.05 \cdot 10^{-2}$ in our**
282 **study. For the men group, this value was measured from $2 \cdot 10^{-2}$ to $25.3 \cdot 10^{-2}$ Mpa vs**
283 **from $10.15 \cdot 10^{-2}$ to $93.74 \cdot 10^{-2}$ in our study. From the results presented in this study, re-**
284 **producible material characteristics were observed among the ruptured and pre-**
285 **ruptured aneurysms with similar biomechanical behavior, suggesting a same vulnerable**
286 **status of the aneurysmal wall in a rupture or pre-rupture status. These two behaviors**
287 **were significantly different from the unruptured aneurysms, presenting a rigid tissue. At**
288 the same time, there was no statistical correlation observed between the thickness of the wall,
289 the aneurysm size and the Ruptured/Unruptured aneurysms status. This observation supports
290 the hypothesis that the aneurysm wall vulnerability is directly related to the tissue microstruc-
291 ture²⁵, and not to a progressive wearing of the wall.

292 The evolution of aneurysmal biomechanical properties was modeled by Watton et al. et
293 al.²⁶ who performed numerical simulations of aneurysmal initiation and growth and postulated
294 a degradation model of the elastin layer. Furthermore, a previous histopathology study²⁵ dem-
295 onstrated that prior to rupture, the wall of cerebral aneurysm undergoes morphological
296 changes associated with degeneration and repair.

297 **The main contribution of our study has been to demonstrate a very significant**
298 **biomechanical property difference between pre-rupture or rupture aneurysms with a**
299 **soft tissue and unruptured aneurysm with a Rigid tissue (Fig.6).**

300

300
301
302
303
304
305
306
307
308
309
310
311
312
313
314
315
316
317
318
319
320
321
322
323
324
325
326
327
328
329
330
331
332

Limitation of the study

Because of the surgical resection necessary to obtain these samples, only aneurysms easily and safely accessible were selected, introducing a potential selection bias in this study. Hence, the MCA location was over-represented. There may be also a bias induced by the differences between cases with indication of surgical treatment compared to those indicated for interventional therapy. Nevertheless we observed aneurysm size ranging from 4.2 to 13 mm representing the majority of aneurysms treated to date. Within the statistical limitations of our sample, we could not observe any significant difference in mechanical properties of the aneurysmal wall according to the location. Interestingly, in the patient harboring two aneurysms (aneurysm #10 and #11) in different locations (ICA and MCA, respectively), we observed similar mechanical properties.

Uniaxial strain/stress testing is not representative of the anisotropic behavior of the aneurysm wall in vivo. **Although, bi-axial testing was contemplated in this study, it is technically challenging to carry out. In our experiments the main limitation was the small size of the strips ranging from 1.2 to 8 mm. Work by Toth et al.¹⁵ also confirms that bi-axial testing does not generate reliable and reproducible results.** MacDonald et al.³⁰ investigated the molecular strength of the collagen fibers layers in 4 aneurysms. When comparing directional tissue strength, an anisotropy was demonstrated by a factor of 2. **In our study, aneurysm samples were selected in a meridional direction in both groups demonstrating a difference between ruptured and unruptured aneurysm in this direction. A bi-axial testing of the sample would have been a response to this high level of anisotropy, but these tests were not possible in our experience due to the very small size of the aneurysms.**

Furthermore, the probability of consistently and systematically slicing the aneurysm sample in the weakest direction in the ruptured aneurysms, and the strongest direction in unruptured aneurysms was unfeasible.

Conclusion

Gender stratification was necessary to interpret the biomechanical testing. Within each gender subgroup; ruptured aneurysms presented lower Rigidity than ruptured aneurysms, supporting the hypothesis that there is a change in the biomechanical properties of the aneurysm wall

333 preceding rupture. Secondly, wall thickness was not correlated to ruptured/unruptured status.
334 An Intermediate subgroup of unruptured aneurysms characterized by material properties cor-
335 responding to softer tissue was identified, and associated with multiple well documented risk
336 factors of aneurysm rupture. Further studies about the biomechanical properties of cerebral
337 aneurysms can help elucidating the biomechanical conditions preceding rupture. With the
338 recent progress in *in vivo* aneurysm wall motion estimation^{17,31} it may be possible soon to
339 estimate *in vivo* mechanical material properties of cerebral aneurysms^{32,33}. Such biomechani-
340 cal parameters might be themselves good predictors of aneurysm rupture or might be inte-
341 grated within a more comprehensive pipeline for image-based patient-specific simulations of
342 fluid-wall structure interaction that renders a personalized estimate of the presence of vulner-
343 able aneurysmal wall tissue and a potential increased rupture risk.

344

345

345

346

347

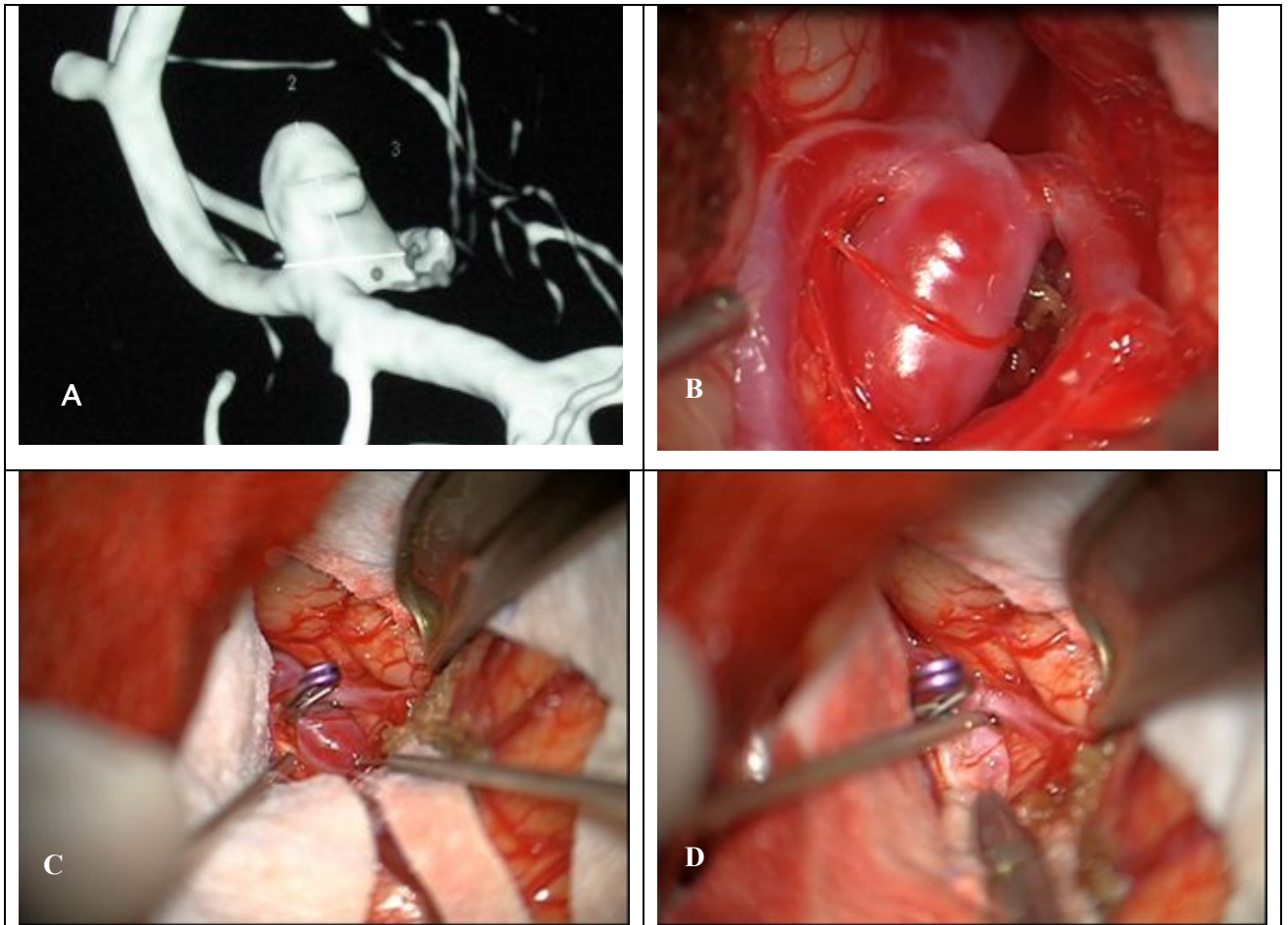


Fig. 1. (A) Three-dimensional rotational angiography imaging from Aneurysm #9. (B) Surgical view of this aneurysm in Middle Cerebral Artery location before clipping. (C) Aneurysm sac after surgical clipping. (D) Aneurysm resection.

348

349

349

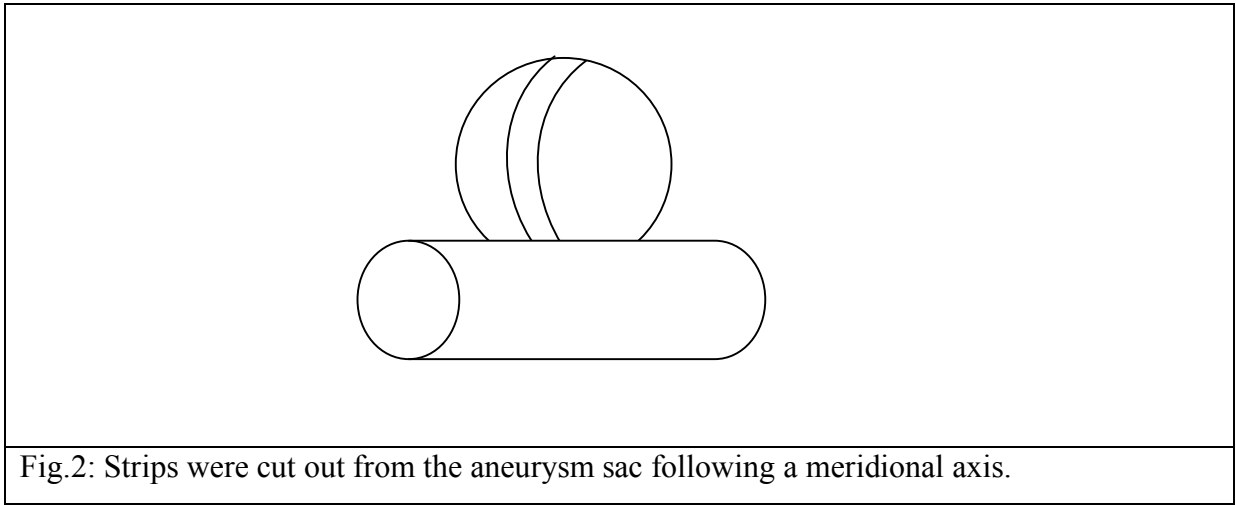
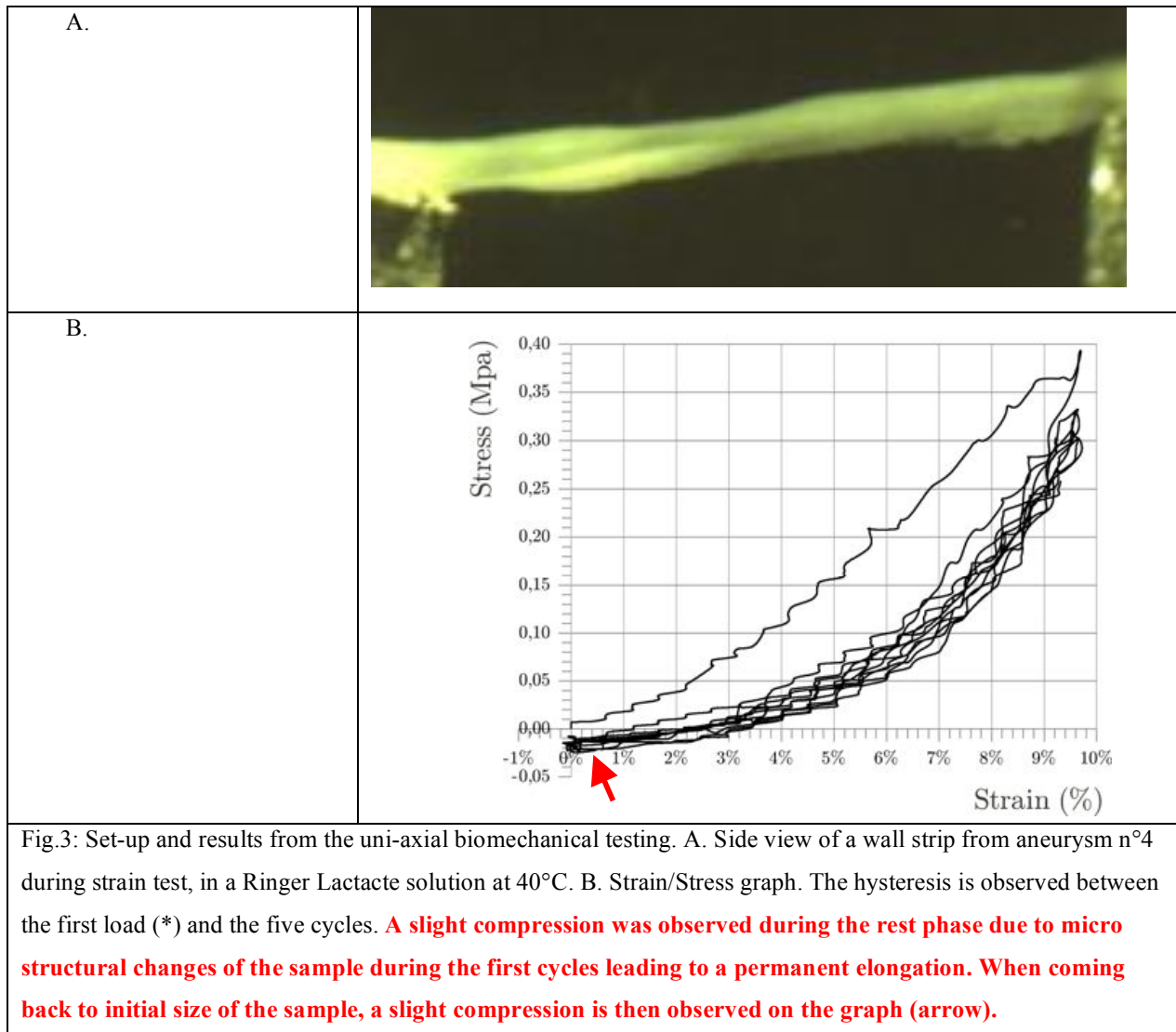


Fig.2: Strips were cut out from the aneurysm sac following a meridional axis.

350

351

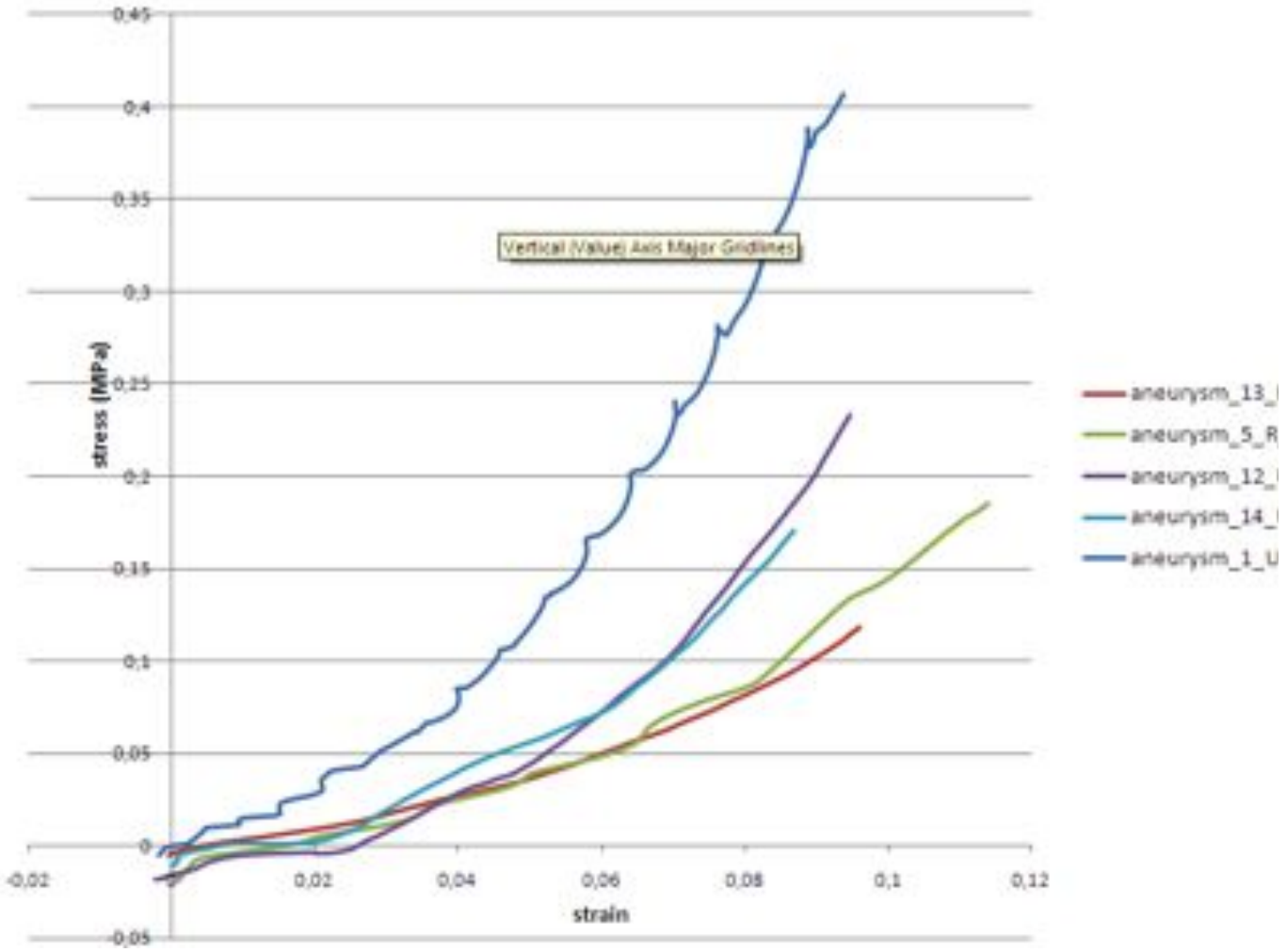


352

353

353
354
355
356

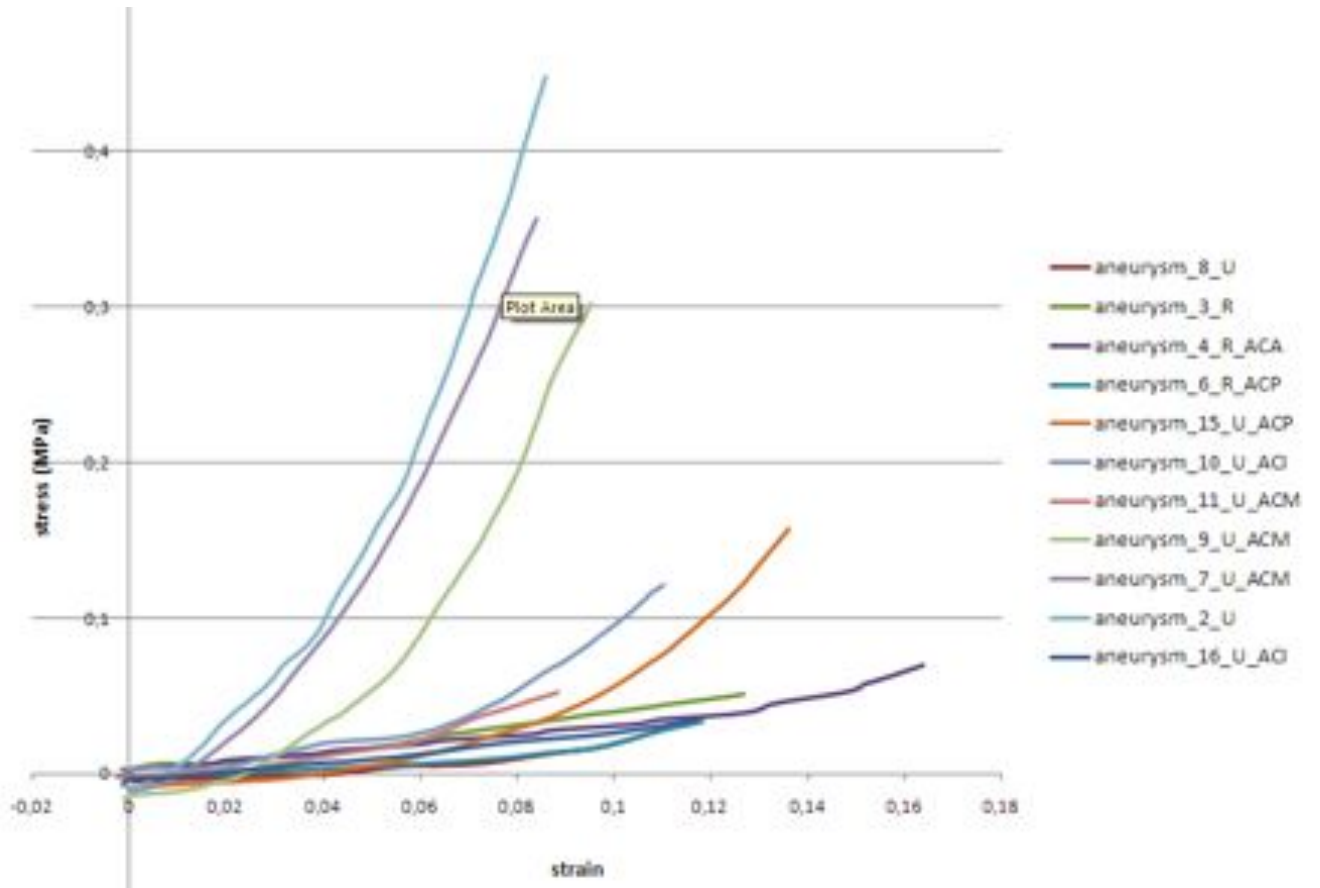
Fig. 4: Plots of the strain/stress relationships measured for men (R=ruptured, U=unruptured, ACA = Anterior Cerebral Artery, ACM=Middle Cerebral Artery)



357
358
359
360
361
362
363
364
365
366
367
368

369
370
371
372
373
374
375

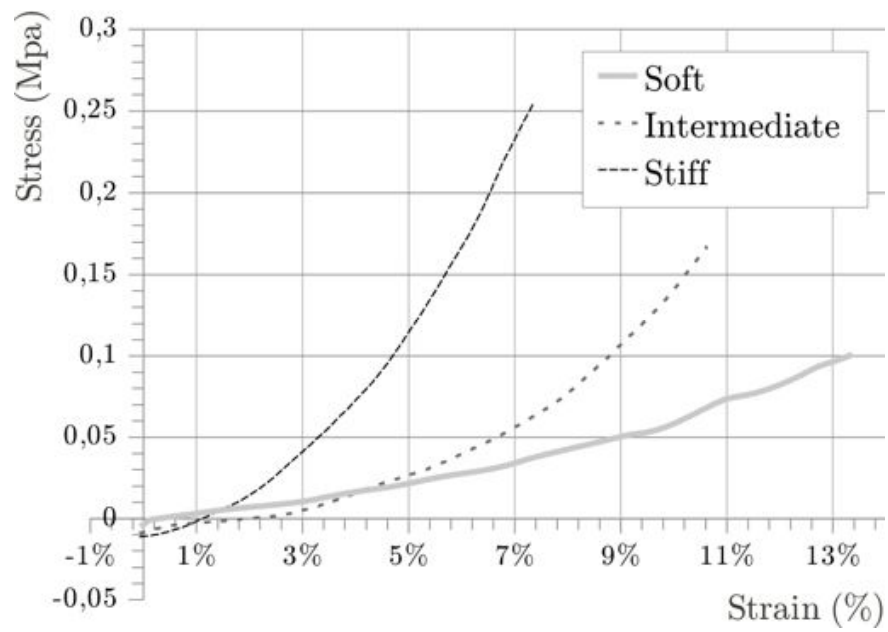
Fig. 5: Plots of the strain/stress relationships measured for women. (R=ruptured, U=unruptured, ACA = Anterior Cerebral Artery, ACM=Middle Cerebral Artery, ACI= Internal Carotid Artery, CPA= Cerebral Posterior Artery)



376
377
378

378

379



380

381 Fig.6: Mean strain/stress curves representing the biomechanical tissue classification.

382

383

383
 384 Table 1: Summary of clinical, anatomical and biomechanical data of the sixteen cases studied.
 385 (U=Unruptured, R=Ruptured, U-PRS = Unruptured with pre-rupture symptoms, MCA
 386 =Middle Cerebral Artery, PComA = Posterior Communicating Artery, ICA = Internal Carotid
 387 Artery).The tissue classification (Soft/Rigid/Intermediate) is done according to the graphs
 388 shown in fig.4 et 5.

389

Female Subgroup	Location	Cumulative Documented Risk Factors	Aneurysm Status	Thickness (µm)	Biomechanical properties	C ₁₀ (MR3) MPa	C ₀₁ (MR3) MPa	C ₁₁ (MR3) MPa	Statistical Error
Aneurysm 3	MCA	0	R	420	Soft	0	0.0639	0.124	0.001
Aneurysm 4	ACA	2	R	300	Soft	0	0.0516	0.23	0.064
Aneurysm 16	ICA	1	U-PRS	380	Soft	0	0.04497	0.3077	0.00465
Aneurysm 6	PCA	5	R	450	Soft	0.02936	0	1.259	0.0355
Aneurysm 8	MCA	2	U	420	Intermediate	0.019057	0	2.196	0.0345
Aneurysm 11	MCA	5	U	390	Intermediate	0.0431	0	2.428	0.039
Aneurysm 10	ICA	5	U	310	Intermediate	0	0.0352	2.482	0.05
Aneurysm 15	PCA	1	U	680	Intermediate	0	0.06582	4.295	0.0433
Aneurysm 2	MCA	1	U	390	Rigid	0.376	0	18.847	0.033
Aneurysm 9	MCA	5	U	260	Rigid	0.2359	-0	19.56	0.049
Aneurysm 7	MCA	1	U	310	Rigid	0.7705	0	32.149	0.0067

390
 391
 392
 393

Male Subgroup	Location	Cumulative Documented Risk Factors	Aneurysm Status	Thickness (µm)	Biomechanical properties	C ₁₀ (MR3) MPa	C ₀₁ (MR3) MPa	C ₁₁ (MR3) MPa	Statistical Error
Aneurysm 5	ACA	1	R	330	Soft	0.1803	0	3.241	0.016
Aneurysm 13	ACA	1	R	290	Soft	0.9374	0	3.101	0.0267
Aneurysm 12	MCA	2	U	170	Intermediate	0.1951	0	14.987	0.0457
Aneurysm 14	MCA	1	U	200	Intermediate	0.1015	0	7.9232	0.04
Aneurysm 1	MCA	1	U	620	Rigid	0.2569	0	12.265	0.035

394
 395
 396
 397

397

398

399

400 **Table 2:** Comparison of clinical and biomechanical parameters between the three identified tissue
401 subgroups in the overall population.

n = 16	Aneurysmal wall biomechanical classification	n	Mean	p
Risk Factors	INTERMEDIATE	6	2.6	0.456
	SOFT	6	1.6	.
	RIGID	4	2	.
Wall Thickness	INTERMEDIATE	6	360	0.994
	SOFT	6	361	.
	RIGID	4	392	.
C10	INTERMEDIATE	6	0.0598	0.057
	SOFT	6	0.1911	.
	RIGID	4	0.3916	.
C01	INTERM	6	0.0168	0.792
	SOFT	6	0.0267	.
	RIGID	4	0.0322	.
C11	INTERM	6	5.71	<.001**
	SOFT	6	1.37	.
	RIGID	4	20.87	.

402

403

404

405

406

407

408

409

410

411

412

413

414

415

416

417

418

419 Table 3: Comparison of clinical data and biomechanical parameters between Ruptured and

420 Unruptured aneurysms in the overall population (male and female).

421

	Status	n	Mean	p
Risk factors	Ruptured	6	1.66	0.366
	Unruptured	10	2.4	.
Wall Thickness	Ruptured	6	0.36	0.918
	Unruptured	10	0,37	.
C10	Ruptured	6	0.19	0.404
	Unruptured	10	0.19	.
C01	Ruptured	6	0.026	0.757
	Unruptured	10	0.023	.
C11	Ruptured	6	1.377	0.004***
	Unruptured	10	11.78	

422

423

423

424

425 Table 4: Comparison of clinical data and biomechanical parameters between Ruptured and
426 Unruptured aneurysms in the female group.

	Status	n	Mean	p
Risk factors	Ruptured	4	2	0.516
	Unruptured	7	2.85	.
Wall Thickness	Ruptured	4	388	0.861
	Unruptured	7	392	.
C10	Ruptured	4	0.00734	0.200
	Unruptured	7	0.20637	.
C01	Ruptured	4	0.04012	0.279
	Unruptured	7	0.01443	.
C11	Ruptured	4	0.48	0.001**
	Unruptured	7	11.70	

427

428

428

429 Table 5: Comparison of clinical data and biomechanical parameters between Ruptured and
430 Unruptured aneurysms in the male group.

	Status	n	Mean	p
Risk factors	Ruptured	2	1	0.495
	Unruptured	3	1.3	.
Wall Thickness	Ruptured	2	309	0.638
	Unruptured	3	329	.
C10	Ruptured	2	0.558	0.638
	Unruptured	3	0.160	.
C01	Ruptured	2	-0.0001	0.638
	Unruptured	3	0.043	.
C11	Ruptured	2	3.17	0.058
	Unruptured	3	11.95	.

431

432

433

434

435

436

437

438

439

440

441

442

443

444

445

446

447

448

449

450

451 **REFERENCES:**

452

- 453 1. Wardlaw JM, White PM. The detection and management of unruptured intracranial
454 aneurysms. *Brain*. 2000;123 (Pt 2):205-221
- 455 2. Sluzewski M, Bosch JA, van Rooij WJ, Nijssen PC, Wijnalda D. Rupture of intracranial
456 aneurysms during treatment with Guglielmi detachable coils: Incidence, outcome, and risk
457 factors. *J Neurosurg*. 2001;94:238-240
- 458 3. Unruptured intracranial aneurysms--risk of rupture and risks of surgical intervention.
459 International study of unruptured intracranial aneurysms investigators. *N Engl J Med*.
460 1998;339:1725-1733
- 461 4. Asari S, Ohmoto T. Natural history and risk factors of unruptured cerebral aneurysms.
462 *Clin Neurol Neurosurg*. 1993;95:205-214
- 463 5. Wiebers DO, Whisnant JP, Sundt TM, Jr., O'Fallon WM. The significance of unruptured
464 intracranial saccular aneurysms. *J Neurosurg*. 1987;66:23-29
- 465 6. Kyriacou SK, Humphrey JD. Influence of size, shape and properties on the mechanics of
466 axisymmetric saccular aneurysms. *J Biomech*. 1996;29:1015-1022
- 467 7. Isaksen JG, Bazilevs Y, Kvamsdal T, Zhang Y, Kaspersen JH, Waterloo K, Romner B,
468 Ingebrigtsen T. Determination of wall tension in cerebral artery aneurysms by numerical
469 simulation. *Stroke*. 2008;39:3172-3178
- 470 8. Alnaes MS, Isaksen J, Mardal KA, Romner B, Morgan MK, Ingebrigtsen T. Computation
471 of hemodynamics in the circle of Willis. *Stroke*. 2007;38:2500-2505
- 472 9. Cebal JR, Castro MA, Appanaboyina S, Putman CM, Millan D, Frangi AF. Efficient
473 pipeline for image-based patient-specific analysis of cerebral aneurysm hemodynamics:
474 Technique and sensitivity. *IEEE Trans Med Imaging*. 2005;24:457-467
- 475 10. Radaelli AG, Augsburg L, Cebal JR, Ohta M, Rufenacht DA, Balossino R, Benndorf G,
476 Hose DR, Marzo A, Metcalfe R, Mortier P, Mut F, Reymond P, Socci L, Verheghe B,
477 Frangi AF. Reproducibility of haemodynamical simulations in a subject-specific stented
478 aneurysm model--a report on the virtual intracranial stenting challenge 2007. *J Biomech*.
479 2008;41:2069-2081
- 480 11. Hoi Y, Meng H, Woodward SH, Bendok BR, Hanel RA, Guterman LR, Hopkins LN.
481 Effects of arterial geometry on aneurysm growth: Three-dimensional computational fluid
482 dynamics study. *J Neurosurg*. 2004;101:676-681
- 483 12. Cebal JR, Mut F, Weir J, Putman C. Quantitative characterization of the hemodynamic
484 environment in ruptured and unruptured brain aneurysms. *AJNR Am J Neuroradiol*.
485 2011;32:145-151
- 486 13. Cebal JR, Mut F, Weir J, Putman CM. Association of hemodynamic characteristics and
487 cerebral aneurysm rupture. *AJNR Am J Neuroradiol*. 2011;32:264-270
- 488 14. Scott S, Ferguson GG, Roach MR. Comparison of the elastic properties of human
489 intracranial arteries and aneurysms. *Can J Physiol Pharmacol*. 1972;50:328-332
- 490 15. Toth BK, Nasztanovics F, Bojtár I. Laboratory tests for strength parameters of brain
491 aneurysms. *Acta Bioeng Biomech*. 2007;9:3-7
- 492 16. Masson I, Fialaire-Legendre A, Godin C, Boutouyrie P, Bierling P, Zidi M. Mechanical
493 properties of arteries cryopreserved at -80 degrees C and -150 degrees C. *Med Eng Phys*.
494 2009;31:825-832
- 495 17. Karmonik C, Diaz O, Grossman R, Klucznik R. In-vivo quantification of wall motion in
496 cerebral aneurysms from 2d cine phase contrast magnetic resonance images. *Rofo*.
497 2010;182:140-150
- 498 18. Ogden GAHaRW. Biomechanical modelling at the molecular, cellular and tissue levels.
499 *CISM Courses and Lectures, Springer: Wien, New York*. 2009;No. 508: 259-343
- 500 19. Marc André Meyers P-YC, Albert Yu-Min Lin, Yasuaki Seki. Biological materials:
501 Structure and mechanical properties, review article. *Progress in Materials Science*.
502 2008;Volume 53:1-206

- 503 20. Oliver A, Shergold NAFaDR. The uniaxial stress versus strain response of pig skin and
504 silicone rubber at low and high strain rates. *International Journal of Impact Engineering*.
505 2006;Volume 32:1384-1402
- 506 21. Mooney M. A theory of large elastic deformation. *Journal of Applied Physics*.
507 1940;11:582-592.
- 508 22. Rivlin RS. Large elastic deformations of isotropic materials. I. *Fundamental concepts*,
509 *Philosophical Transactions of the Royal Society of London. Series A, Mathematical and*
510 *Physical Sciences*. 1948; 240:459-490.
- 511 23. Low SK, Zembutsu H, Takahashi A, Kamatani N, Cha PC, Hosono N, Kubo M, Matsuda
512 K, Nakamura Y. Impact of limk1, mmp2 and tnf-alpha variations for intracranial
513 aneurysm in japanese population. *J Hum Genet*. 2011
- 514 24. Crawford T. Some observations on the pathogenesis and natural history of intracranial
515 aneurysms. *J Neurol Neurosurg Psychiatry*. 1959;22:259-266
- 516 25. Frosen J, Piippo A, Paetau A, Kangasniemi M, Niemela M, Hernesniemi J, Jaaskelainen J.
517 Remodeling of saccular cerebral artery aneurysm wall is associated with rupture:
518 Histological analysis of 24 unruptured and 42 ruptured cases. *Stroke*. 2004;35:2287-2293
- 519 26. Watton PN, Ventikos Y, Holzapfel GA. Modelling the growth and stabilization of cerebral
520 aneurysms. *Math Med Biol*. 2009;26:133-164
- 521 27. Krings T, Willems P, Barfett J, Ellis M, Hinojosa N, Blobel J, Geibprasert S. Pulsatility of
522 an intracavernous aneurysm demonstrated by dynamic 320-detector row cta at high
523 temporal resolution. *Cen Eur Neurosurg*. 2009;70:214-218
- 524 28. Hayakawa M, Katada K, Anno H, Imizu S, Hayashi J, Irie K, Negoro M, Kato Y, Kanno
525 T, Sano H. Ct angiography with electrocardiographically gated reconstruction for
526 visualizing pulsation of intracranial aneurysms: Identification of aneurysmal protuberance
527 presumably associated with wall thinning. *AJNR Am J Neuroradiol*. 2005;26:1366-1369
- 528 29. Ishida F, Ogawa H, Simizu T, Kojima T, Taki W. Visualizing the dynamics of cerebral
529 aneurysms with four-dimensional computed tomographic angiography. *Neurosurgery*.
530 2005;57:460-471; discussion 460-471
- 531 30. MacDonald DJ, Finlay HM, Canham PB. Directional wall strength in saccular brain
532 aneurysms from polarized light microscopy. *Ann Biomed Eng*. 2000;28:533-542
- 533 31. Zhang C, Villa-Uriol MC, De Craene M, Pozo JM, Frangi AF. Morphodynamic analysis of
534 cerebral aneurysm pulsation from time-resolved rotational angiography. *IEEE Trans Med*
535 *Imaging*. 2009;28:1105-1116
- 536 32. Balocco S, Camara O, Vivas E, Sola T, Guimaraens L, Gratama van Andel HA, Majoie CB,
537 Pozo JM, Bijnens BH, Frangi AF. Feasibility of estimating regional mechanical properties
538 of cerebral aneurysms in vivo. *Med Phys*. 2010;37:1689-1706
- 539 33. Zhao X, Raghavan ML, Lu J. Identifying heterogeneous anisotropic properties in cerebral
540 aneurysms: A pointwise approach. *Biomech Model Mechanobiol*. 2011;10:177-189

541

542

543

543

544

545 **Conflict of interest statement**

546 All authors do not have any financial and personal relationships with other people or organi-

547 sations that could inappropriately influence this work.

548

549

549

550 **Acknowledgement:**

551 The authors would like to thank Philips™, Ansys™, for funding part of this research and pro-
552 viding free research software licenses. These sources of funding were not involved in the
553 study design, in the collection, analysis and interpretation of data; in the writing of the manu-
554 script; and in the decision to submit the manuscript for publication.

555